

ESPL1 is Elevated in Hepatocellular Carcinoma and Predicts Prognosis

Rui Song^{1,2,*}, Juntao Huang^{1,2,*}, Chenglei Yang^{1,2}, Yuankuan Li^{1,2}, Guohua Zhan^{1,2}, Bangde Xiang^{1-3,*}

¹Department of Hepatobiliary Surgery, Guangxi Medical University Cancer Hospital, Nanning, People's Republic of China; ²Key Laboratory of Early Prevention and Treatment for Regional High-Frequency Tumors, Ministry of Education, Nanning, People's Republic of China; ³Guangxi Liver Cancer Diagnosis and Treatment Engineering and Technology Research Center, Nanning, People's Republic of China

*These authors contributed equally to this work

Correspondence: Bangde Xiang, Department of Hepatobiliary Surgery, Guangxi Medical University Cancer Hospital, 71 Hedi Road, Qingxiu District, Nanning, Guangxi, 530021, People's Republic of China, Tel +86-7715301253, Email xiangbangde@gxmu.edu.cn

Purpose: The extra spindle pole bodies-like 1 (*ESPL1*) gene is associated with malignant biological behaviors in several tumors. Nevertheless, the correlation between hepatocellular carcinoma (HCC) and *ESPL1* has not been determined. The present study analyzed the molecular function and prognostic value of *ESPL1* in HCC.

Patients and Methods: Samples from 121 HCCs and 119 adjacent normal tissue specimens were subjected to next-generation sequencing. Clinicopathological and genetic data of HCC patients in The Cancer Genome Atlas (TCGA) were also collected. *ESPL1* expression was assessed in 20 pairs of HCC and normal liver specimens by qRT-PCR and immunohistochemistry (IHC). The prognostic value of *ESPL1* expression was determined by Cox univariate and multivariate regression analyses. *ESPL1*-related co-expressed genes were evaluated by weighted gene co-expression network analysis (WGCNA). Processes and pathways involving *ESPL1* in HCC were determined by Gene Ontology (GO) enrichment and Kyoto Encyclopedia of Genes and Genomes (KEGG) pathway analyses. The prognostic values of hub genes were determined by joint effect survival analysis.

Results: RNA-Seq, RT-qPCR and IHC showed that *ESPL1* expression was significantly higher in HCC than in normal liver tissues. Increased *ESPL1* expression, greater tumor size and advanced BCLC stage were independently prognostic of poorer overall survival; and increased *ESPL1* and advanced BCLC stage were independently prognostic of poorer recurrence-free survival. WGCNA showed that the top 10 co-expressed genes associated with *ESPL1* were *GTSE1*, *KIF18B*, *BUB1B*, *GINS1*, *PRC1*, *KIF23*, *KIF18A*, *TOP2A*, *NEK2* and *FANCD2*. Enrichment analysis indicated that *ESPL1* and its co-expressed genes might be involved in the cell cycle and cell division of HCC. Joint effect survival analysis showed that the mortality rate was approximately 3.37 times higher in HCC patients with high than low expression of *ESPL1*, *GTSE1*, *BUB1B*, *PRC1*, *KIF23*, and *TOP2A*.

Conclusion: *ESPL1* might be associated with cell cycle and might be an effective prognostic indicator in patients with HCC.

Keywords: hepatocellular carcinoma, extra spindle pole bodies-like 1, prognosis

Introduction

Hepatocellular carcinoma (HCC) is the sixth most frequent type of cancer worldwide, with the third highest mortality rate.¹ Although surgery is regarded as the most effective treatment for patients with HCC, the high incidence of tumor relapse after surgery can negatively affect post-treatment outcomes and survival.^{2,3} Tumor recurrence within 5 years after surgery, has been observed in 70% of HCC patients worldwide.⁴ Furthermore, tumor heterogeneity contributes to increased tumor resistance to conventional chemotherapy and targeted therapies.⁵ Identification of new prognostic biomarkers and therapeutic targets may improve clinical outcomes in patients with HCC.

The extra spindle pole bodies-like 1 (*ESPL1*) gene encodes a protein involved in the cell cycle. The *ESPL1* protein is primarily involved in the anaphase process of sister chromatid cohesion release by cleaving the mucin subunit *SCC1*, which initiates the final separation of sister chromatids.⁶ *ESPL1* expression is elevated and predicts poor outcomes in patients with various types of cancer, including breast cancer,⁷ glioma⁸ and endometrial cancer.⁹ A Chinese case-control

study found that the level of *ESPL1* was higher in HBV-associated than in non-HBV-associated HCC, suggesting that serum *ESPL1* can be a biomarker of HCC recurrence in HBV-associated HCC.¹⁰ To date, however, the genetic aspects and molecular function of *ESPL1* in HCC have not yet been investigated.

The present study assessed whether *ESPL1* can act as a prognostic marker in patients with HCC. Samples from the Guangxi cohort and The Cancer Genome Atlas (TCGA) were subjected to next-generation sequencing to determine the level of expression, prognostic value, and biological function of *ESPL1* and its encoded. Total RNA was isolated from HCCs and adjacent normal tissue samples, and *ESPL1* mRNA levels were evaluated by real-time quantitative-polymerase chain reaction (qRT-PCR), Protein expression detected by IHC. This study showed that high expression of *ESPL1* was associated with a poorer prognosis in patients with HCC, suggesting that *ESPL1* may be a promising biomarker and a treatment target in patients with HCC.

Materials and Methods

Clinical Tissue Specimens

HCC and adjacent normal liver tissue samples for next-generation sequencing were collected from 121 patients who had been pathologically diagnosed with HCC and had undergone tumor resection at the Hepatobiliary Surgery unit of Guangxi Medical University Cancer Hospital from April 2018 to July 2019. There were no restrictions with respect to age and sex. HCC patients were excluded if they had other co-occurring tumors, had very little tumor tissue, had received preoperative radiotherapy and/or chemotherapy, or refused to provide written informed consent. Twenty additional pairs of HCC and adjacent normal liver tissue samples were also collected for qRT-PCR and IHC validation. The study protocol was approved by the Ethics Committee of the Cancer Hospital of Guangxi Medical University and conformed to the principles of the Helsinki Declaration. All patients provided written informed consent for their anonymized data to be analyzed for research purposes.

RNA-seq

Frozen samples of 121 HCCs and 119 adjacent normal tissues were subjected to RNA sequencing. Each tissue sample was added to an EP tube containing 1 mL of MagZol Reagent (Trizol lysis solution) to extract total RNA. Integrity of each total RNA sample, expressed as RNA integrity number (RIN), was subsequently determined using a 2100 Bioanalyzer (Agilent) analyzer, and the absorbances of each RNA sample at 260 nm and 280 nm were measured using an Epoch 2 microplate spectrophotometer. The screening standards included an OD_{260/280} ratio between 1.9 and 2.0 and an RIN ≥ 4 . Cytoplasmic and mitochondrial rRNA were removed from each total RNA sample using Ribo-Zero™ Magnetic Gold Kit (Human). Each RNA sample was randomly cleaved into short template fragments of 200–500 bp and reversed transcribed to yield a cDNA library. The concentration of each cDNA sequencing library was measured by Qubit 2.0 dsDNA HS Assay (Thermo Fisher Scientific). Finally, the cDNA library samples were subjected to DNA analysis using an Agilent BioAnalyzer 2100, with the distribution of cDNA fragments analyzed by agarose gel electrophoresis. Each cDNA library was sequenced on an Illumina HiSeq 2000 high-throughput sequencer using a 2×150 paired-end sequencing protocol (Illumina), with the original sequencing data obtained in FASTQ format.

RNA-seq Data Quality Control and Analysis

Quality-controlled raw data were matched with the sequence of a human reference genome (gencode hg19) using the sequence alignment software Hisat. Exons of different genes were alternatively spliced to yield the final RNA sequence for each sample, and the measured clean reads were compared with the annotation information of the human reference genome, based on the number of reads that uniquely matched a gene and all reads that uniquely matched the reference genome sequence quantity, thus determining the levels of expression of all genes matched on all samples. Theoretically, the number of reads aligned for a single gene correlated positively with the expression of that gene. During the actual calculation process, however, quantitative gene expression was found to be closely related with sequencing depth and gene length. Therefore, the actual level of expression of each gene was determined by a normalization method using the algorithm FPKM. Differentially

expressed genes (DEGs) in tumors and adjacent normal tissues were screened using the “DESeq2” package of R software, with a $|\log_2 \text{fold change}|$ ($|\log_2 \text{FC}|$) ≥ 0.6 and adjusted $P < 0.05$ regarded as the threshold.

qRT-PCR

Total RNA was extracted from HCC and adjacent normal tissues using TRIzol reagent (TaKaRa, Japan), followed by reverse transcription of RNA into cDNA (Monad, China). *ESPL1* mRNA was quantified using an SYBR Green Master kit (Hieff, China) and the specific primers 5'-ATCTCTGTCAGTCGGACCTGCA-3' (forward) and 5'-CAGGTGGACCTTCTTCACAGAG-3' (reverse); as a loading control, the same cDNA samples were subjected to qRT-PCR using primers for β -actin, 5'-GTCATTCCAAATATGAGATGCGT-3' (forward) and 5'-GCTATCACCTCCCCTGTGTG-3' (reverse). All PCR amplifications were performed using the AriaMx Real-time PCR System (Agilent, USA), with the amplification protocol consisting of an initial denaturation at 95°C for 5 min, followed by 40 cycles of denaturation at 95°C for 10s, annealing at 62°C for 15s, and extension at 72°C for 20s. The relative expression of *ESPL1* mRNA to β -actin mRNA was determined using the $2^{-\Delta\Delta C_t}$ method.

Immunohistochemistry Analysis

We used IHC analysis to verify the expression of *ESPL1* in HCC and adjacent tissues at the protein level. Collected tissue specimens were formalin fixed and embedded with paraffin. Tissue sections (4 μm thickness) were used in IHC staining analyses. The sections were deparaffinized in xylene and rehydrated by graded ethanol. Antigen retrieval was carried out using sodium citrate buffer (pH 6.0) at 95°C for 20 minutes. After quenching endogenous peroxidase activity with 3% H₂O₂ and blocking non-specific binding with 1% bovine serum albumin buffer. The sections were incubated with primary anti-*ESPL1* antibody (Sigma-Aldrich, SAB4503690, Saint Louis, USA) at 1:100 dilution and incubation at 37 °C for 80 minutes. Sections were incubated with secondary antibody (MaxVision™ HRP-Polymer anti-Mouse/Rabbit IHC Kit, KIT-5030, Fuzhou, China) for 25 minutes at room temperature, finally, stained with diaminobenzidine (MaxVision, DAB-1031, Fuzhou, China).¹¹ IHC outcomes were assessed through two pathologists who were blinded to group allocation, and all differences were resolved through discussion.

Genomic Data Mining

Independent sets of genomic data and clinical parameters were collected from The Cancer Genome Atlas (TCGA, <https://tcga-data.nci.nih.gov> accessed February 10, 2022), a public database. Data were obtained from the Gene Expression Profiling Interactive Analysis (GEPIA) webserver (<http://gepia.cancer-pku.cn/index.html>; accessed February 10, 2022),¹² and the correlations among gene expression patterns, tumor stages and the ability of *ESPL1* expression to predict survival outcomes were analyzed in patients with HCC. In addition, data on the expression of *ESPL1* protein in HCC and adjacent normal tissues were obtained from the Human Protein Atlas (HPA, <https://www.proteinatlas.org/>; accessed March 1, 2022).¹³ The mutation frequency of the *ESPL1* gene was assessed in the cBioPortal database¹⁴ (<http://www.cbioportal.org/>, accessed March 1, 2022). Drug sensitivity associated with the *ESPL1* gene was analyzed in the Genomics of Drug Sensitivity in Cancer (GDSC) database and immune cell infiltration of HCCs associated with the *ESPL1* gene by Gene Set Cancer Analysis (GSCA, <https://www.proteinatlas.org/>, accessed March 2, 2022).¹⁵ The single-cell sequencing data of six HCCs¹⁶ were obtained from the Tumor Immune Single-cell Hub (TISCH, <http://tisch.comp-genomics.org/home/>).¹⁷ We entered the type of cancer and the name of the gene in the “dataset” option and the results of the single cell analysis were generated.

Weighted Gene Co-expression Network Analysis

Based on the median expression of *ESPL1* mRNA, patients with HCC were classified into high and low expression groups. Differences in gene expression between these two groups were determined using “DESeq2” to screen DEGs, with $\log_2 \text{fold changes}$ $|\log_2 \text{FC}| > 1$ and adjusted $P < 0.05$ set as the threshold. Weighted gene co-expression network analysis (WGCNA) was performed to identify *ESPL1*-related co-expressed DEGs that formed the *ESPL1* gene co-expression network. Briefly, a soft threshold power with a scale-free $R^2 > 0.9$ and a slope near 1 was selected to transform the adjacency matrix to a topological overlap matrix. To establish networks and identify modules, the minimum size of the module was set at 30, the cutting height at 0.25, and the soft threshold power at 3. Highly similar modules were merged to create a compression network. The correlations of modules and clinical parameters

with the *ESPL1* gene were determined. In addition, the genes in each module with high connectivity in the weighted co-expression network were selected, and the Pearson correlation coefficients of gene expression with clinical parameters were calculated as gene significance (GS). Generally, modules with higher values showed more powerful correlations with *ESPL1* and clinical parameters. Modules that correlated significantly with *ESPL1* were considered interested modules, with modules identified as having key genes when their $|MM| > 0.8$ and their $|GS| > 0.4$. The biological processes and enrichment pathways associated with key genes in the interested modules were analyzed using GO and KEGG.

Hub Gene Identification and Prognostic Analysis

Genes of weight >0.2 in the WGCNA modules that correlated significantly with *ESPL1* were entered into Cytoscape software (version 3.8.2) to further analyze PPI networks and select hub genes.¹⁸ Using the cytoHubba plugin in Cytoscape, the top 10 hub genes in the *ESPL1* gene-related module were selected and visualized by the Degree method. A prognostic scoring model based on gene prognostic contribution coefficients (β) was also determined,¹⁹ and the predictive prognostic ability of these genes was validated using the TCGA dataset.

Statistical Analysis

Statistical analyses were performed using R 4.1.0 (<https://www.r-project.org/>) or SPSS 22.0 (IBM, Armonk, NY, USA) software, with P -values <0.05 considered statistically significant. Each clinical parameter was evaluated by univariate and multivariate Cox regression analyses. Differences between groups were analyzed by paired or unpaired Student's t -tests. All graphics were visualized using PRISM8.3.0 (Graph Pad, San Diego, CA, USA) and R 4.1.0.

Results

ESPL1 is Frequently Upregulated in HCC and Regulates the Cell Cycle

Tissue samples were obtained from 121 patients with HCC in the Guangxi cohort, including from 121 tumors and 119 adjacent normal tissue samples. These 121 patients included 105 (86.8%) men and 16 (13.2%) women, of mean age 50.6 years, who were followed-up for a median 25 months (Table 1). For validation, 374 patients with HCC in the TCGA dataset were analyzed, with data obtained from 374 tumor tissues and 50 adjacent normal tissues. After excluding patients whose survival time was 0 or unknown, 365 patients were analyzed, with data obtained from 365 tumors and 50 adjacent normal tissue samples. These 365 patients included 246 (67.3%) men and 119 (32.7%) women, of mean age 59.6 years, who were followed-up for a median 19.8 months (Table S1).

RNA-seq analysis showed that *ESPL1* mRNA expression was markedly higher in HCC samples than in adjacent normal tissue and increased as differentiation worsened and BCLC stages progressed (Figures 1A–D). For validation, *ESPL1* mRNA expression was assessed by qRT-PCR in 20 pairs of samples obtained from patients with HCC who underwent resection at our hospital. Consistent with the RNA-seq data, *ESPL1* mRNA expression was higher in HCC samples than in adjacent normal tissue (Figure 1E). Similar results were obtained in the TCGA cohort (Figure S1).

Immunohistochemistry also confirmed that the expression of *ESPL1* was significantly upregulated in HCC tissues compared with normal liver tissues (Figures 2A and E). *ESPL1* was mainly expressed in the nucleus, cytoplasm or both. Furthermore, immunofluorescence staining showed that *ESPL1* was mainly expressed in the nucleoplasm of three cell lines, the human skin squamous cell carcinoma (A-431), human osteosarcoma (U2-OS) and human glioma (U-251 MG) cell lines (Figure 2B). *ESPL1* expression increased sequentially during the cell cycle, from G1 to S transition (S-tr) to the S and G2 phases, being highest in the S and G2 phases, suggesting that *ESPL1* may promote tumor development by accelerating the process of DNA synthesis (Figures 2C and D).

ESPL1 Overexpression is Associated with Poorer Outcome

A comparison of HCC patients with high and low *ESPL1* mRNA expression showed that high expression of *ESPL1* in HCC was associated with poorer survival outcomes (Figure 3). Multivariate Cox regression analysis showed that high *ESPL1* expression (hazard ratio [HR] =2.004, $P=0.032$), larger tumor size (HR=2.468, $P=0.021$), and more advanced

Table I Clinical Baseline Characteristics of HCC Patients in Our Cohort

Variable	N (%)
Sex	
Male	105 (86.8%)
Female	16 (13.2%)
Age (years)	
≤65	108 (89.3%)
>65	13 (10.7%)
BCLC stage	
0-A	62 (51.2%)
B-C	59 (48.8%)
Edmondson grade	
I-II	60 (49.6%)
III-IV	57 (47.1%)
Missing ^a	4 (3.3%)
Tumor size	
≤5cm	39 (32.2%)
>5cm	82 (67.8%)
Cirrhosis	
Positive	49 (40.5%)
Negative	64 (52.9%)
Missing ^b	8 (6.6%)
HbsAg	
Positive	101 (83.5%)
Negative	20 (16.5%)
AFP (ng/mL)	
≤400	75 (62.0%)
>400	46 (38.0%)

Notes: ^aMissing information of Cirrhosis was unknown in 4 patients; ^bMissing information of Cirrhosis was unknown in 8 patients.

Abbreviations: BCLC stage, Barcelona Clinic Liver Cancer; AFP, alpha-fetoprotein; ESPL1, extra spindle pole bodies-like 1.

BCLC stage (HR=1.956, $P=0.038$) were independent risk factors for poorer overall survival (Table 2). In addition, high *ESPL1* expression (HR=1.653, $P=0.036$) and more advanced BCLC stage (HR=2.217, $P=0.002$) were independent risk factors for poorer recurrence-free survival (RFS). High expression of *ESPL1* mRNA (HR=1.757, $P=0.005$) was also an independent risk factor for poorer OS in the TCGA cohort (Table S2).

ESPL1 Related Gene Co-Expression and Prognostic Analysis

The network of genes co-expressed with *ESPL1* genes was assessed by WGCNA analysis. A weighted gene network was constructed, with 3 selected as the threshold β of a suitable adjacency matrix; this threshold satisfied the criterion that the network was close to scale-free (Figure 4A). Subsequently, five modules were identified via the merged dynamic (Figure 4B). The association of modules with *ESPL1* was assessed using a heatmap (Figure 4D), with the results suggesting that the blue model was most positively associated with *ESPL1* mRNA expression ($r=0.89$, $P<0.001$) (Figure 4C), whereas the green, brown and red modules were negatively correlated with *ESPL1* mRNA expression. In the blue model, genes associated with the cell cycle and cell division pathways were significantly enriched in analyses of the GO and KEGG (Figure 5, Tables S3 and S4). This enabled the identification of the top 10

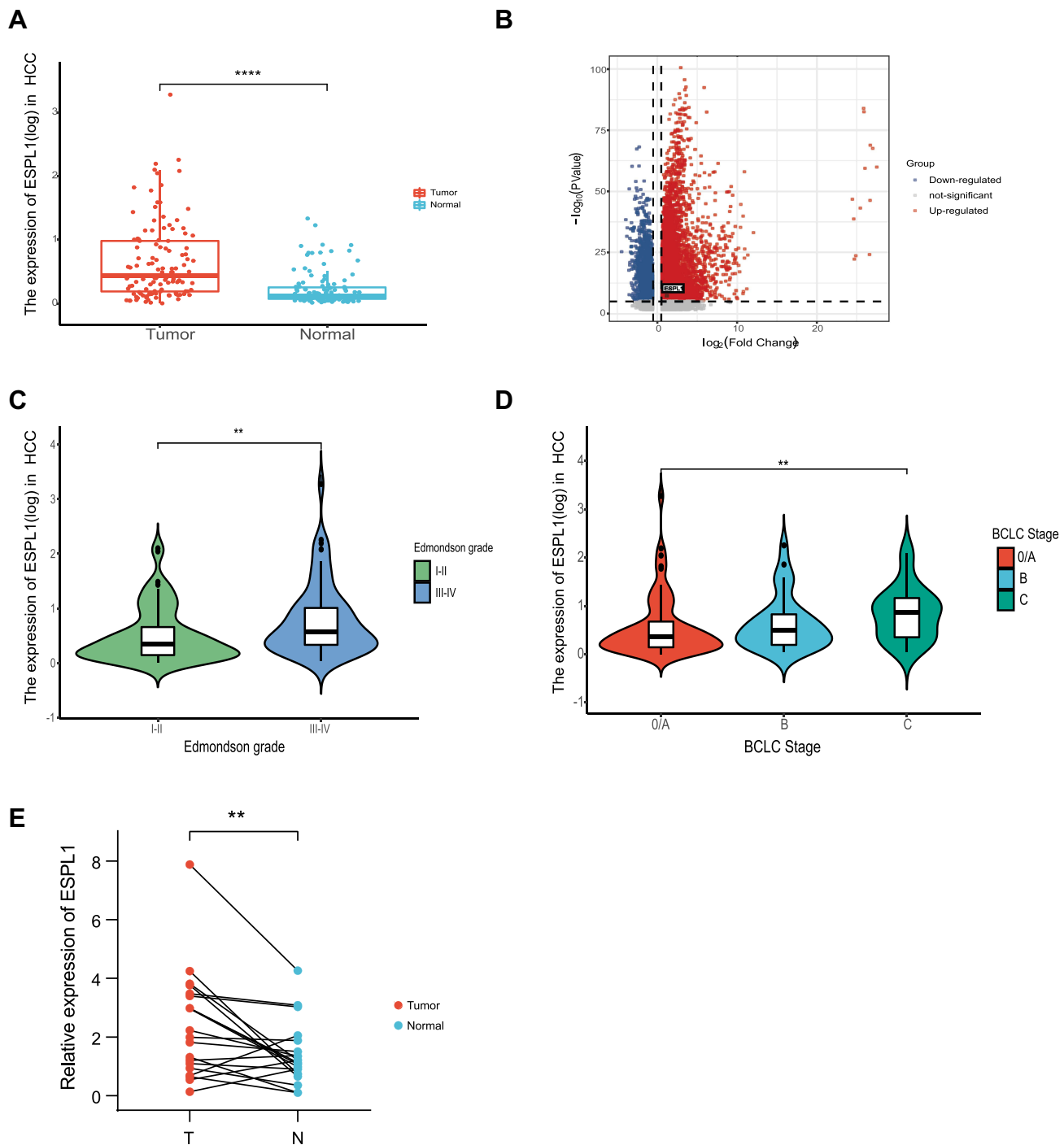


Figure 1 *ESPL1* mRNA expression in HCC in the Guangxi RNA-seq database. **(A and B)** *ESPL1* expression levels in tumors and adjacent normal tissues. **(C and D)** Association between *ESPL1* expression and clinical characteristics. **(E)** qRT-PCR validation of *ESPL1* expression in tumor tissues and adjacent normal tissues. **** $P < 0.0001$; ** $P < 0.01$; * $P < 0.05$.

Abbreviations: T, tumor tissues; N, normal tissues; BCLC, Barcelona-Clinic Liver Cancer; *ESPL1*, extra spindle pole bodies-like 1; HCC, hepatocellular carcinoma.

hub genes of the blue model, including *GTSE1*, *KIF18B*, *BUB1B*, *GINS1*, *PRC1*, *KIF23*, *KIF18A*, *TOP2A*, *NEK2*, and *FANCD2* (Figure 4E).

The prognostic value of the top 10 *ESPL1*-related co-expressed hub genes was also investigated in HCC samples. The multivariate survival analysis included BCLC stage, Edmondson grade, age, tumor size and AFP concentration as adjusted prognostic factors. After adjustment, poorer OS was found to be significantly associated with high levels of

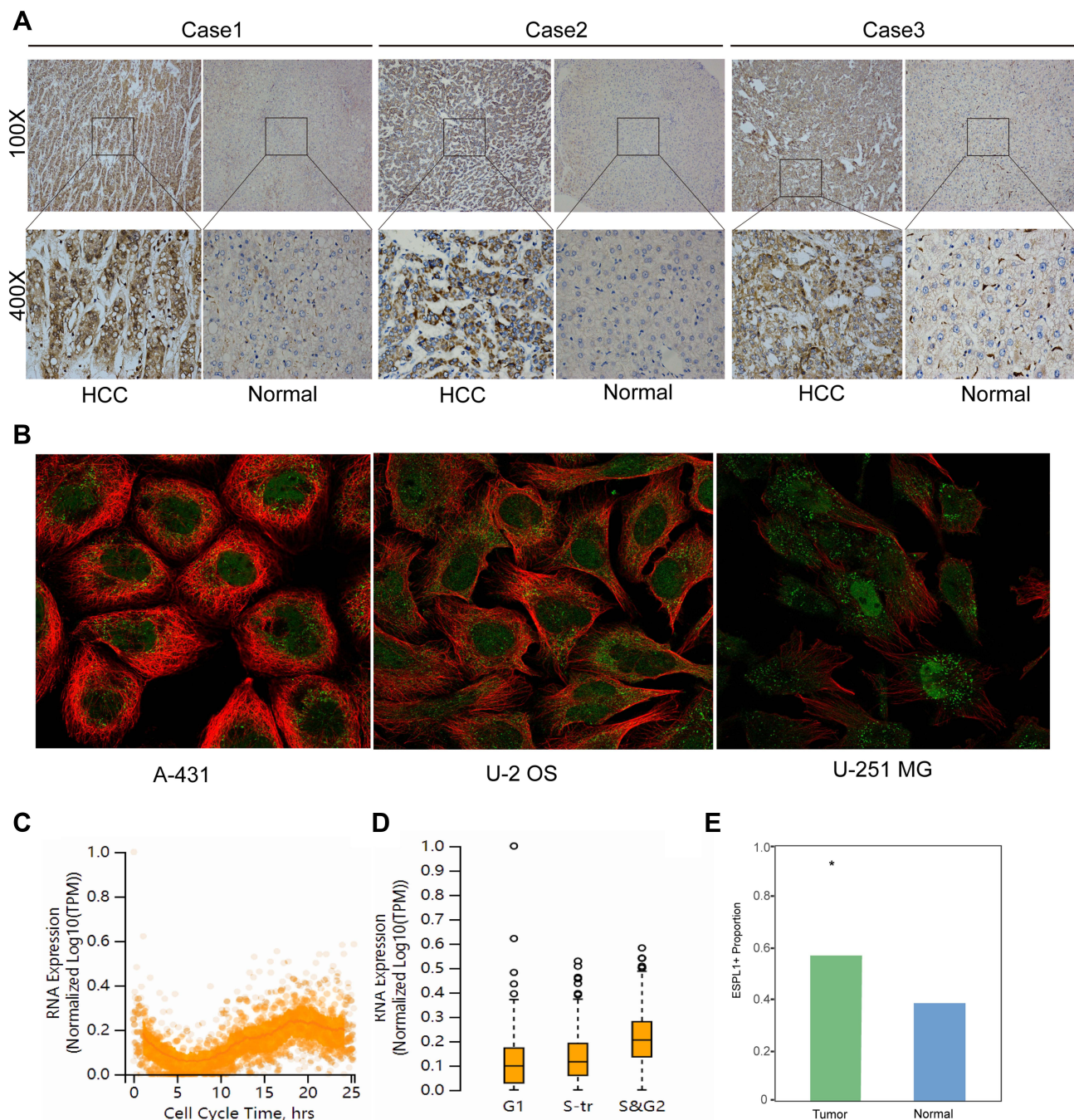


Figure 2 ESPL1 protein is greatly expressed in HCC samples. (**A** and **E**) Immunohistochemical staining of HCC tissue samples and adjacent normal tissues. (Magnification, 100× and 400×; *P < 0.05.) (**B**) Immunofluorescent staining of human epidermoid carcinoma (A-431), osteosarcoma (U-2-OS) and glioblastoma (U-251 MG) cell lines in the HPA database. The red color represents microtubule and the green color represents ESPL1. (**C** and **D**) ESPL1 expression level and cell cycle phase in single U-2 OS cells. **Abbreviations:** HPA, the human protein atlas; HCC, hepatocellular carcinoma.

expression of the genes G-2 and S-phase expressed 1 (*GTSE1*), BUB1B mitotic checkpoint serine/threonine kinase B (*BUB1B*), protein regulator of cytokinesis 1 (*PRC1*), kinesin family member 23 (*KIF23*) and DNA topoisomerase II alpha (*TOP2A*) (Figures 6A–F Table 3). Joint effect prognostic analysis found that the mortality rate was approximately 3.376 times higher in HCC patients with high than low expression of *ESPL1*, *GTSE1*, *BUB1B*, *PRC1*, *KIF23* and *TOP2A* (Table 4 and Figure 6G).

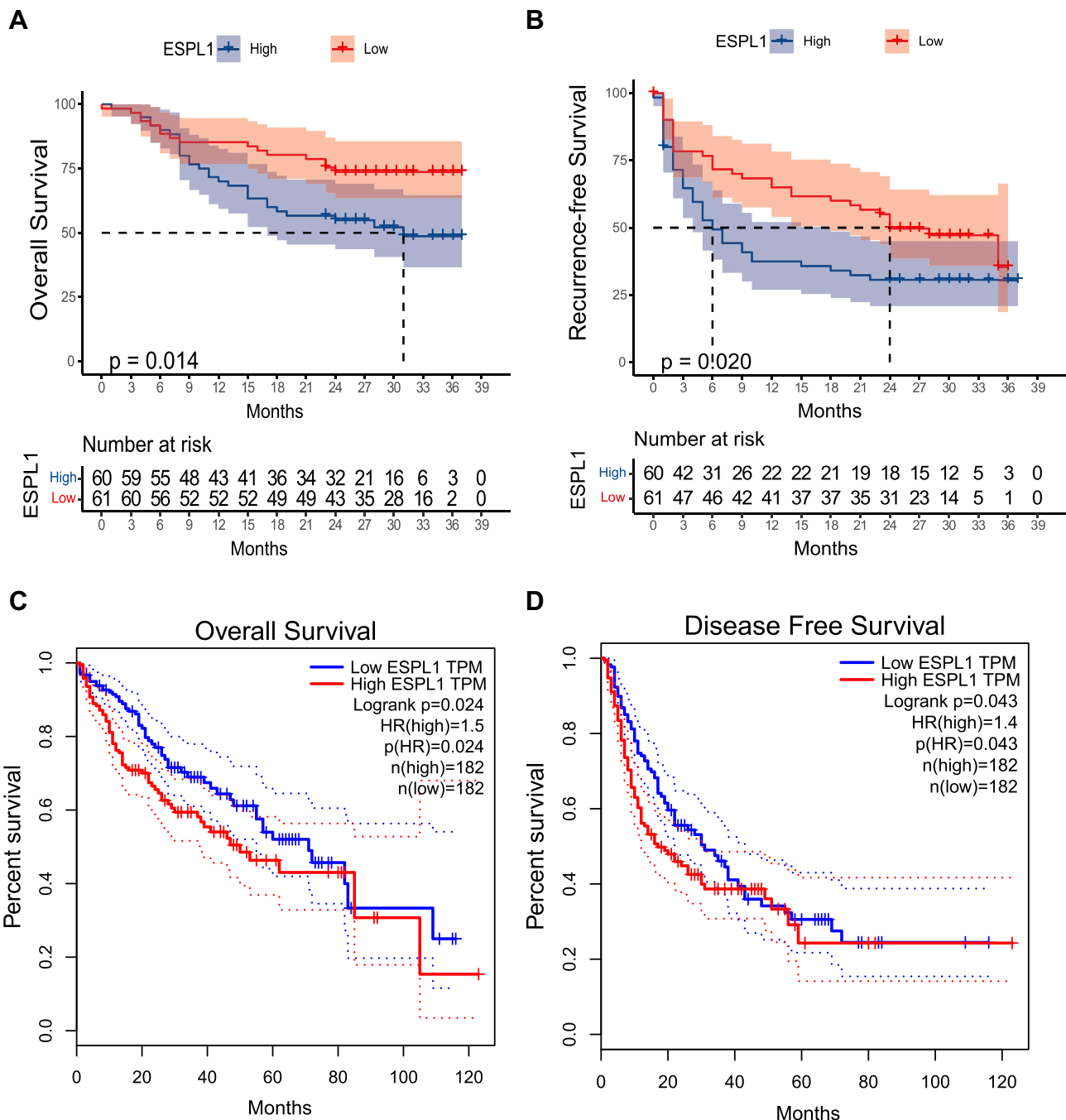


Figure 3 Effects of *ESPL1* mRNA expression level on survival in patients with HCC. Relationship of *ESPL1* mRNA with OS (**A** and **C**) and RFS (**B** and **D**) in the (**A** and **B**) Guangxi cohort and (**C** and **D**) the GEPIA database.

Abbreviations: *ESPL1*, extra spindle pole bodies-like 1; OS, overall survival; RFS, recurrence-free survival; GEPIA, gene expression profiling interactive analysis; HCC, hepatocellular carcinoma.

Based on the median risk score, the 121 patients with HCC were divided into high- and low-risk groups. Kaplan-Meier analysis showed that OS was significantly lower in HCC patients with high than low risk scores (Figure 7A and B). Time-dependent receiver operating characteristic (ROC) curve analysis showed that the 1-, 2-, and 3-year areas under the curve (AUCs) were 0.71, 0.72 and 0.72, respectively (Figure 7C). Validation of the prognostic model in the TCGA dataset also showed that OS was significantly lower in the high-risk than in the low-risk group (Figure 7D and E), with time-dependent ROC curve analysis showing that the 1-, 2-, and 3-year AUCs were 0.74, 0.67 and 0.64, respectively (Figure 7F).

Table 2 Univariate and Multivariate Analysis of OS and RFS in HCC Patients Based on Our Cohort

Variable	OS				RFS			
	Univariate		Multivariate		Univariate		Multivariate	
	HR (95% CI)	P	HR (95% CI)	P	HR (95% CI)	P	HR (95% CI)	P
<i>ESPL1</i> (high)	2.105 (1.141–3.882)	0.017	2.004 (1.072–3.743)	0.032	1.692 (1.063–2.693)	0.027	1.653 (1.032–2.645)	0.036
Sex (Male)	1.341 (0.529–3.398)	0.537			1.063 (0.529–2.138)	0.863		
Age (>65years)	0.525 (0.162–1.694)	0.281			0.529 (0.213–1.315)	0.170		
Tumor size (>5cm)	2.628 (1.223–5.644)	0.013	2.468 (1.137–5.354)	0.021	1.552 (0.933–2.582)	0.091		
BCLC Stage (B-C)	2.424 (1.302–4.504)	0.005	1.956 (1.037–3.692)	0.038	2.468 (1.528–3.987)	<0.001	2.217 (1.348–3.646)	0.002
Cirrhosis (Positive)	0.809 (0.432–1.516)	0.509			0.971 (0.603–1.563)	0.903		
HBsAg (Positive)	1.326 (0.561–3.133)	0.521			1.395 (0.716–2.720)	0.328		
AFP (>400ng/mL)	1.504 (0.837–2.701)	0.172			1.610 (1.014–2.557)	0.044	1.347 (0.833–2.177)	0.225

Abbreviations: 95% CI, 95% confidence interval; HR, hazards ratio. OS, overall survival; RFS, recurrence-free survival; BCLC stage, Barcelona Clinic Liver Cancer; AFP, alpha-fetoprotein.

Relationship of *ESPL1* Expression with Drug Sensitivity

ESPL1 gene expression was positively correlated with sensitivity to the drugs 17-AAG, RDEA119, and Trametinib (Figures S2A and S2B). Moreover, the *ESPL1* mutation rate in HCC was 7% (Figure S2C).

ESPL1 is Enriched in Proliferating T Cells

The mechanisms underlying the biological effects of *ESPL1* in HCC were further evaluated in scRNA-seq data. Proliferating T cells (Tprolif) were identified by their expression of ProlifMKI67, TOP2A and TYMS^{20,21} (Figure S3). *ESPL1* was found to be clustered in the subset of Tprolif cells (Figures 8A–D). Consistent with the results of bulk RNA-seq data, enrichment analysis based on the hallmark database suggested that *ESPL1* was involved in mitotic spindle formation, the G2M checkpoint and DNA repair (Figures 8E–G).

Discussion

HCC is one of the most prevalent malignant tumors worldwide. Various factors are involved in the development of hepatocellular carcinoma, including chronic viral infections,²² changes in the immune microenvironment²³ and abnormalities in metabolism.^{24,25} Samples from HCC patients admitted to Guangxi Medical University Cancer Hospital were subjected to next-generation sequencing, with these findings validated by qRT-PCR, IHC and in the TCGA database. In both the Guangxi and TCGA cohorts, *ESPL1* were higher in tumors than in adjacent normal tissue samples, these findings are consistent with the results studies showing that the overexpression of *ESPL1* was associated with the progression of other tumor types.^{7–9,26} In contrast, reduced expression of *ESPL1* was associated with the progression of gastric carcinoma.²⁷ Taken together, these findings show that the expression of *ESPL1* varies among tumor types, but is more highly expressed in most tumors than in adjacent normal tissues. Clinically, *ESPL1* overexpression correlated with poor outcomes and advanced tumor stages in patients with HCC, suggesting that *ESPL1* level may predict tumor progression. In addition, univariate and multivariate survival analyses indicated that *ESPL1* may be a promising biomarker for the prognosis of patients with HCC.

Analysis of genes co-expressed with *ESPL1* indicated their involvement in cell cycle pathways, mitotic sister chromatid segregation, and HCC cell division. CDKs are often upregulated in cancer cells to allow easier progression through the cell cycle,²⁸ suggesting that treatment with drugs that inhibit CDKs may be a novel therapeutic strategy.²⁹ The top 10 co-expressed genes were included in prognostic analyses, with the results suggesting that enhanced expression of six genes, *ESPL1*, *GTSE1*, *BUB1B*, *PRC1*, *KIF23* and *TOP2A*, may be associated with poor prognosis in patients with HCC.

GTSE1 is expressed specifically during the G2 and S phases of the cell cycle and may be a key regulator involved in mitosis.³⁰ High *GTSE1* expression is associated with poor prognosis in patients with breast cancer and HCC, and may enhance tumor cell proliferation and metastasis by upregulating the expression of EMT markers.^{31–33} *PRC1*,

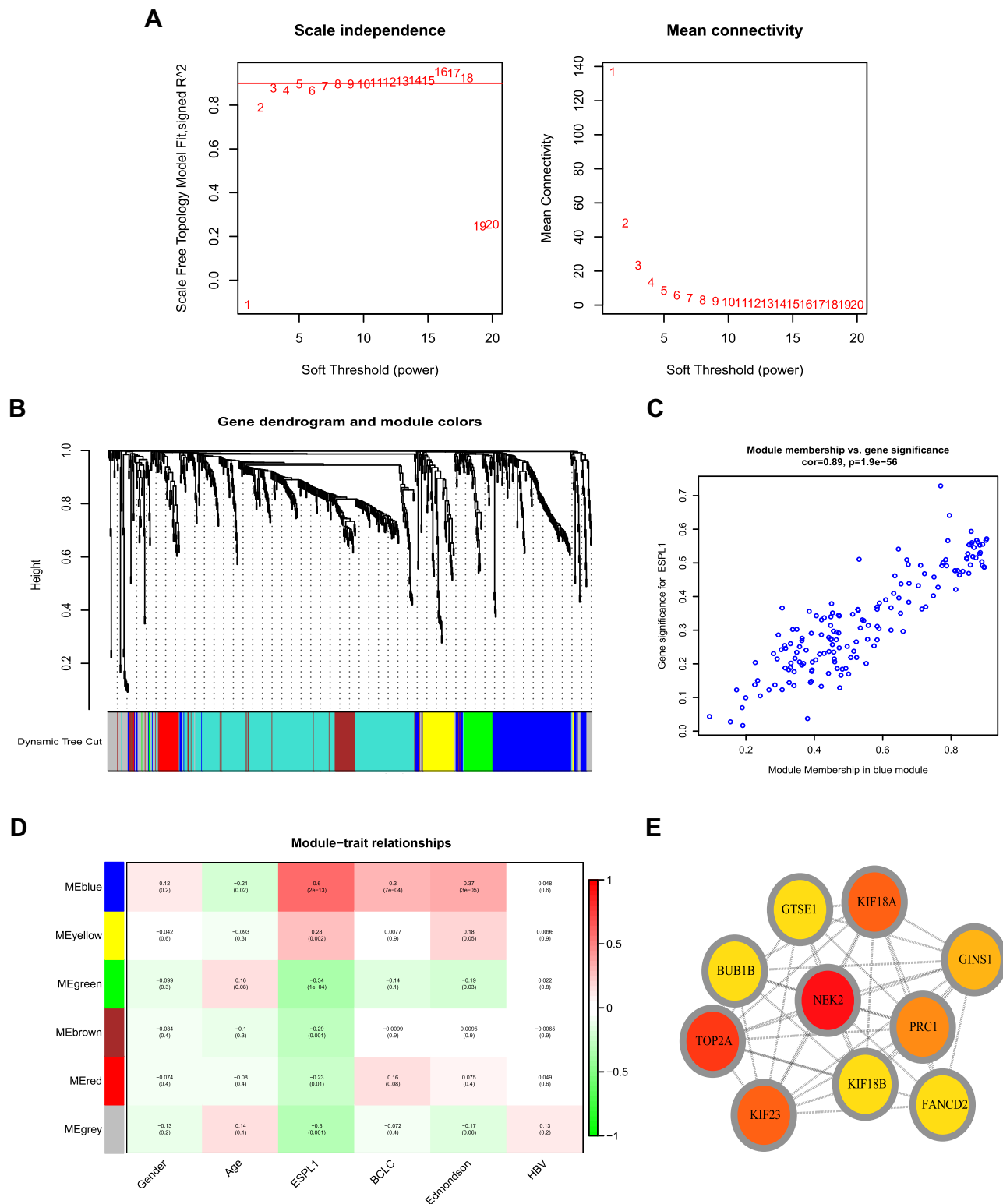


Figure 4 WGCNA analysis of: **(A)** network topology for various soft-thresholding powers (weighted coefficient, β). The x-axis represents different soft-thresholding powers. The y-axis represents the correlation coefficient between $\log(k)$ and $\log[P(k)]$. The red line indicates a correlation coefficient of 0.9. **(B)** Clustering gene dendrogram showing five co-expressed modules (different colors) in patients with HCC. **(C)** Scatter plot of gene and module correlation within the blue module. **(D)** Heatmap showing the relationships between modules and clinical parameters; the correlation coefficient and corresponding P-value are shown in each cell. **(E)** Top 10 genes in the blue module.

Abbreviations: WGCNA, weighted correlation network analysis; HCC, hepatocellular carcinoma.

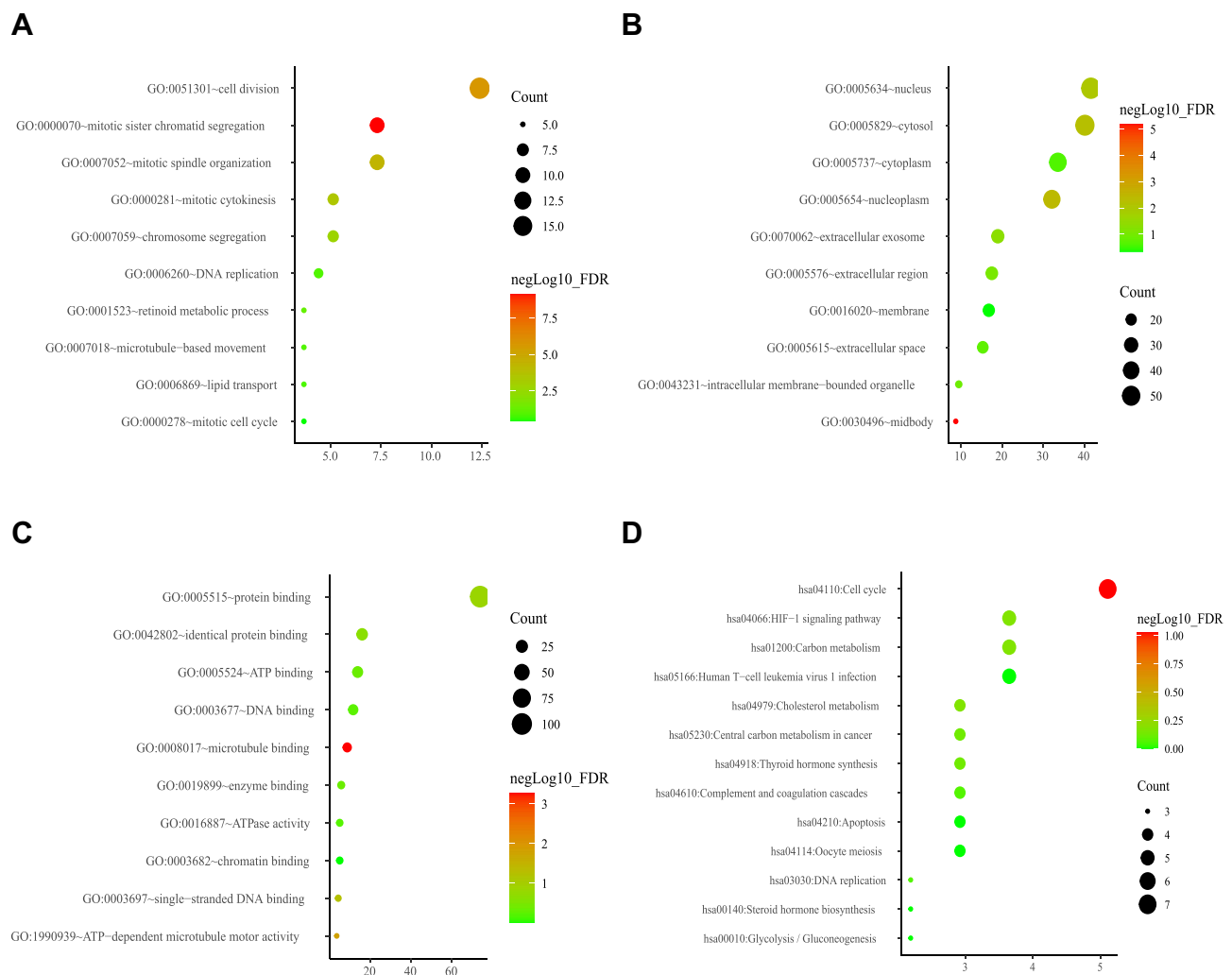


Figure 5 Enrichment analysis of GO and KEGG ontologies and pathways among DEGs in the blue module (**A**) GO-BP; (**B**) GO-CC; (**C**) GO-MF; (**D**) KEGG. **Abbreviations:** GO-BP, Gene Ontology-Biological Process; GO-CC, Gene Ontology-Cellular Component; GO-MF, Gene Ontology-Molecular Function; KEGG, Kyoto Encyclopedia of Genes and Genomes.

a microtubule-associated protein involved in cytokinesis, is overexpressed in various cancers, including pancreatic,³⁴ breast³⁵ and bladder³⁶ cancers. PRC1 exerts an oncogenic effect on HCC by promoting cancer cell proliferation, stemness, metastasis and oncogenesis. Mechanistically, PRC1 can reinforce the Wnt signaling pathway to promote early HCC recurrence.³⁷ KIF23 is a type of nuclear protein that has been shown critical in modulating cytokinesis. Dysregulated expression of *KIF23*, leading to poorer outcomes, has been observed in various cancers,^{38–41} indicating that *KIF23* overexpression is widely associated with tumor progression. *TOP2A* is an essential nuclear enzyme that regulates the state of DNA during transcription and participates in processes of chromatid separation.⁴² *TOP2A* is also expressed in tumor tissues, with elevated expression of *TOP2A* in non-muscle-invasive bladder cancer being indicative of tumor progression and a high rate of recurrence.⁴³ *TOP2A* is also involved in many other important biological behaviors—such as cell proliferation and invasion—which play pivotal roles in tumor initiation and progression, including in bladder urothelial carcinoma,⁴⁴ ovarian cancer⁴⁵ and HCC.⁴⁶ In general, the prognostic model based on the six aberrantly expressed genes identified in the present study may be predictive of OS in patients with HCC.

The cell cycle is a regular and tightly regulated biological process that consists of four phases, pre-DNA synthesis (G1), DNA replication (S), late DNA synthesis (G2), and mitosis (M). Disruption and dysregulation of the cell cycle can lead to undesirable consequences, such as unlimited cell proliferation and tumors.⁴⁷ The present study found that *ESPL1*

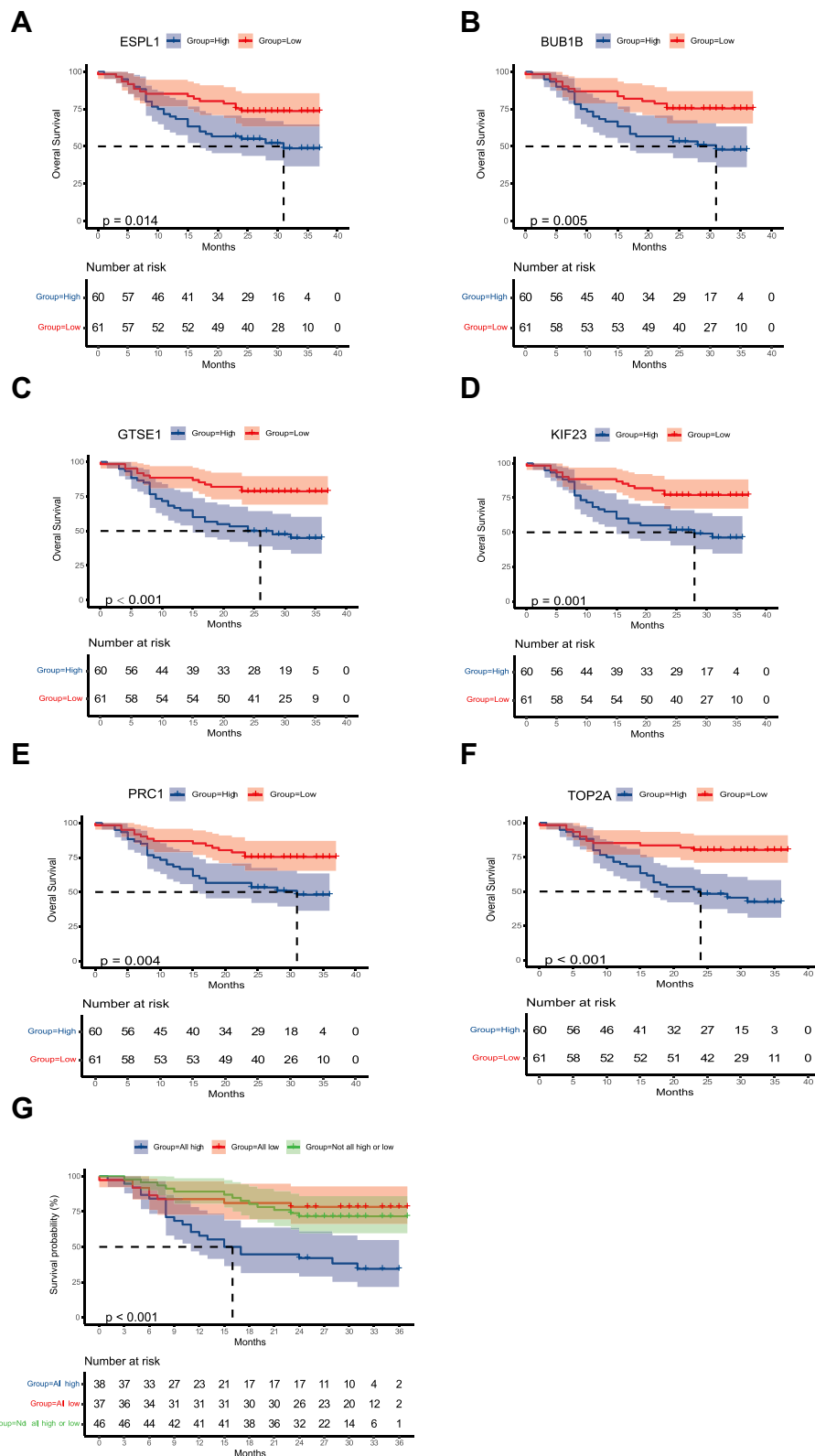


Figure 6 Kaplan–Meier analysis of OS in patients relative to the levels of expression of the genes (A) *ESPL1* (B) *BUB1B* (C) *GTSE1* (D) *KIF23* (E) *PRC1* (F) *TOP2A*. (G) Joint model based on six genes.

Abbreviations: HCC, hepatocellular carcinoma; *ESPL1*, extra spindle pole bodies like 1; *BUB1B*, BUB1 mitotic checkpoint serine/threonine kinase B; *GTSE1*, G-2 and S-phase expressed 1; *KIF23*, kinesin family member 23; *PRC1*, protein regulator of cytokinesis 1; *TOP2A*, DNA topoisomerase II alpha; OS, overall survival.

Table 3 Prognostic Values of Top 10 *ESPL1* Co-Expressed Genes in HCC Based on Our Cohort

Gene	Patients	OS		
	(n=121)	No. of Events	HR (95% CI)	Adjusted P ^a
<i>ESPL1</i>				0.033
Low	61	16	Ref	
High	60	29	2.019 (1.058–3.852)	
<i>GTSE1</i>				0.004
Low	61	13	Ref	
High	60	32	2.732 (1.367–5.459)	
<i>KIF18B</i>				0.055
Low	61	15	Ref	
High	60	30	1.918 (0.987–3.729)	
<i>BUB1B</i>				0.034
Low	61	15	Ref	
High	60	30	2.009 (1.053–3.833)	
<i>GINSI</i>				0.097
Low	61	16	Ref	
High	60	29	1.723 (0.907–3.273)	
<i>PRCI</i>				0.039
Low	61	15	Ref	
High	60	30	1.982 (1.034–3.802)	
<i>KIF23</i>				0.027
Low	61	14	Ref	
High	60	31	2.119 (1.090–4.120)	
<i>KIF18A</i>				0.116
Low	61	16	Ref	
High	60	29	1.687 (0.879–3.237)	
<i>TOP2A</i>				0.001
Low	61	12	Ref	
High	60	33	3.124 (1.547–6.308)	
<i>NEK2</i>				0.136
Low	61	16	Ref	
High	60	29	1.626 (0.858–3.080)	

Note: ^aAdjusted *P*, adjustment for BCLC stage, Edmondson grade, age, tumor size and AFP.

Abbreviations: *ESPL1*, extra spindle pole bodies-like 1; *GTSE1*, genes G-2 and S-phase expressed 1; *KIF18B*, kinesin family member 18B; *BUB1B*, mitotic checkpoint serine/threonine kinase B; *GINSI*, GINS complex subunit 1; *PRCI*, protein regulator of cytokinesis 1; *KIF23*, kinesin family member 23; *KIF18A*, *TOP2A*, DNA topoisomerase II alpha; *NEK2*, NIMA related kinase 2.

Table 4 Joint Effect Survival Analysis

Gene	Patients (n=121)	OS			
		HR (95% CI)	Crude <i>P</i>	HR (95% CI)	Adjusted P ^a
Low <i>ESPL1</i> & <i>GTSE1</i> & <i>BUB1B</i> & <i>PRCI</i> & <i>KIF23</i> & <i>TOP2A</i>	37	Ref		Ref	
Not all high or low	46	1.285 (0.532–3.103)	0.577	1.384 (0.561–3.414)	0.481
High <i>ESPL1</i> & <i>GTSE1</i> & <i>BUB1B</i> & <i>PRCI</i> & <i>KIF23</i> & <i>TOP2A</i>	38	3.742 (1.676–8.358)	<0.001	3.376 (1.463–7.790)	0.004

Note: ^aAdjusted *P*, adjustment for BCLC stage, Edmondson grade, age, tumor size and AFP.

Abbreviations: *ESPL1*, extra spindle pole bodies-like 1; *GTSE1*, genes G-2 and S-phase expressed 1; *KIF18B*, kinesin family member 18B; *BUB1B*, mitotic checkpoint serine/threonine kinase B; *GINSI*, GINS complex subunit 1; *PRCI*, protein regulator of cytokinesis 1; *KIF23*, kinesin family member 23; *KIF18A*, *TOP2A*, DNA topoisomerase II alpha; *NEK2*, NIMA related kinase 2.

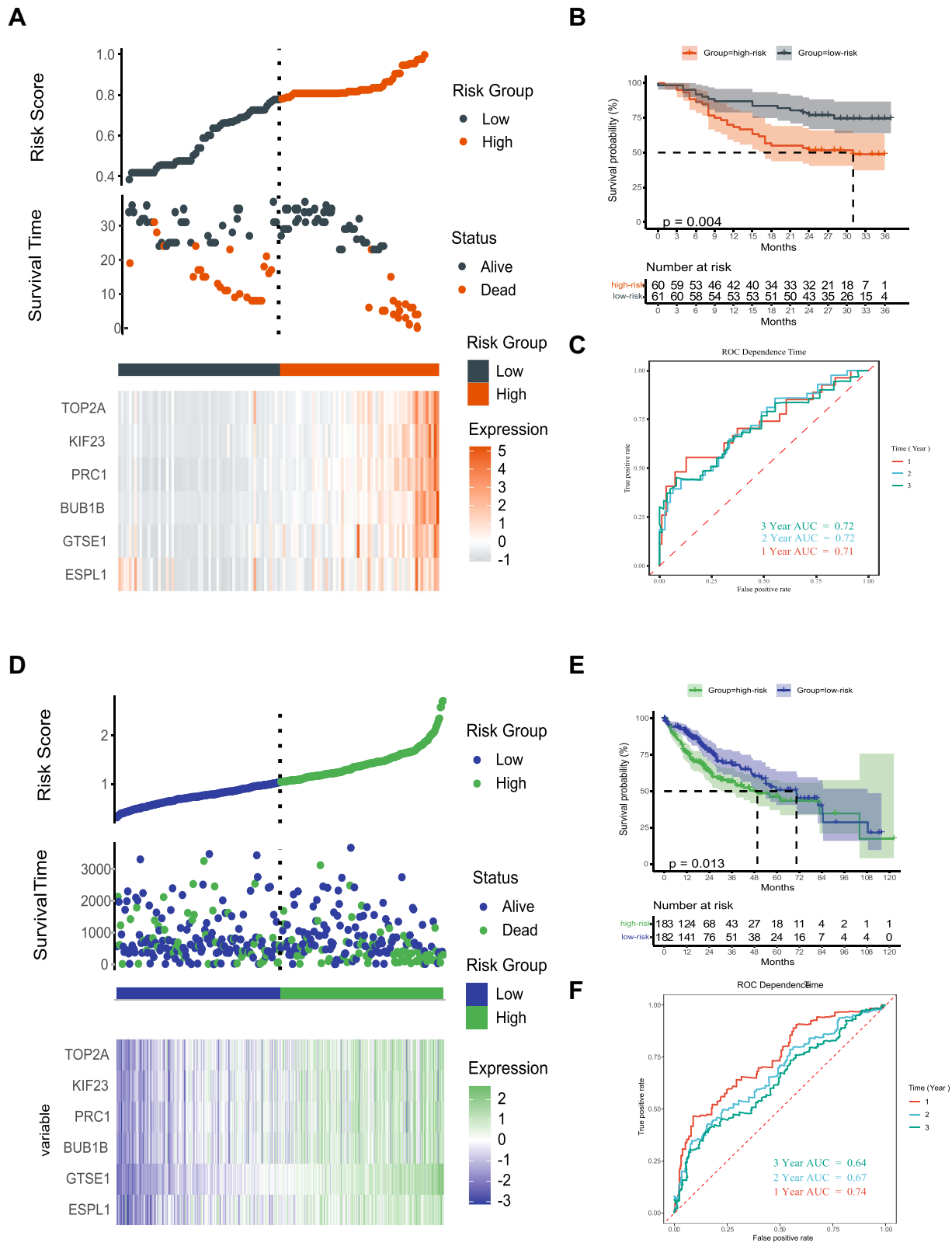


Figure 7 Prognostic risk score model and time-dependent ROC curve of the *ESPL1* gene in HCC (A–C) Guangxi cohort; (D–F) TCGA cohort.

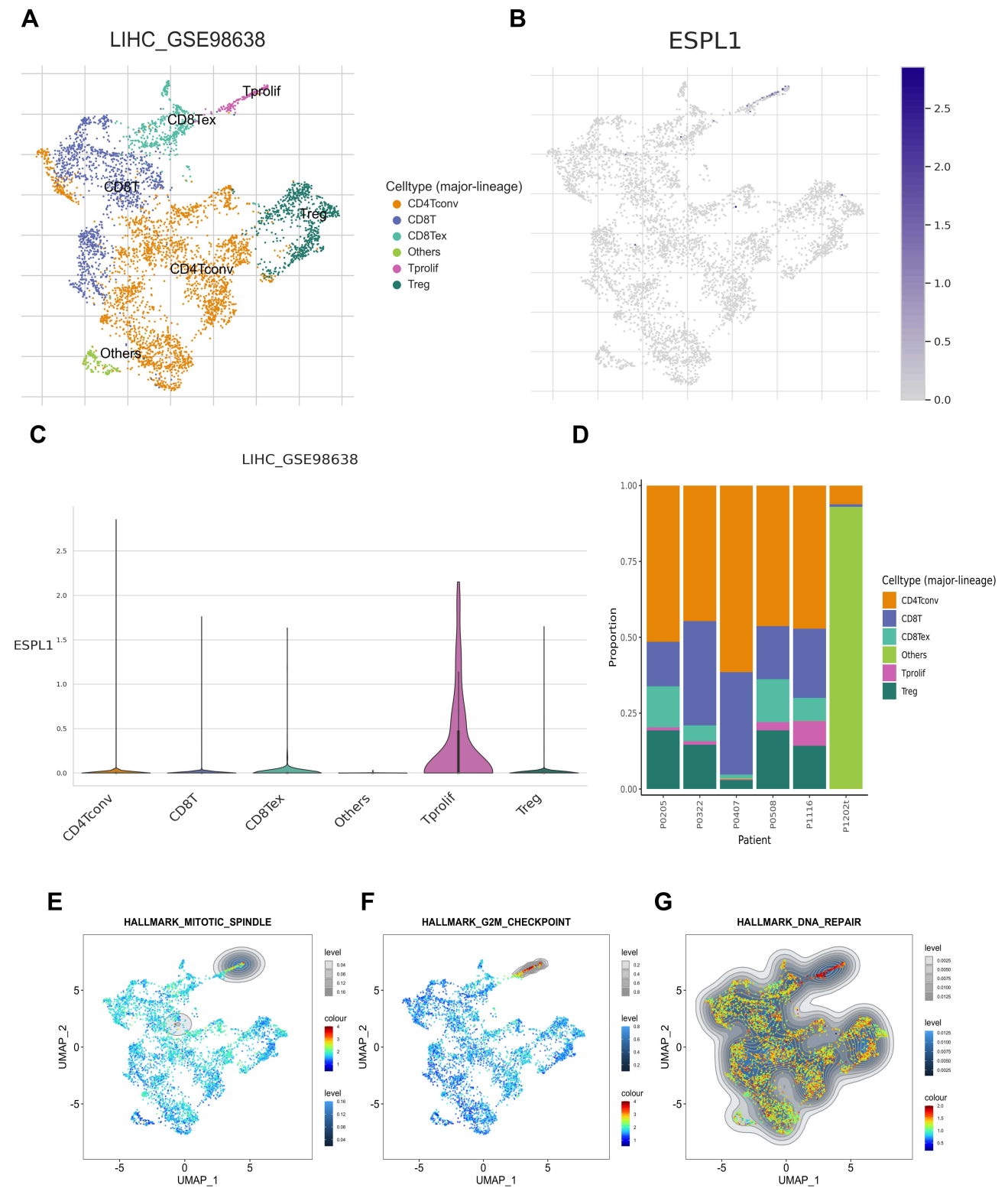


Figure 8 Single cell profiling of six HCCs from the TISCH database. **(A–C)** UMAP and violin plots showing the expression levels of *ESPL1*. **(D)** Proportions of immune cells in tumor tissue of six HCC patients. **(E–G)** Pathway enrichment of proliferating T cells based on the HALLMARK dataset. **Abbreviations:** TISCH, tumor immune single-cell hub; HCC, hepatocellular carcinoma.

expression was highest in S and G2 phases, suggesting that ESPL1 may promote mitosis and tumor proliferation by regulating these phases of the cell cycle.

The present study had several limitations. First, our study suggests that this gene is associated with the cell cycle, but lacks experimental validation. In addition, *in vitro* and *in vivo* experiments are needed to determine the molecular function of ESPL1 and its mechanism of action.

Conclusion

In conclusion, the present study showed that *ESPL1* was associated with cell cycle, cell proliferation and may be an effective prognostic indicator in patients with HCC.

Funding

This work was supported by grants from the National Natural Science Foundation of China (81960450), the High-Level Innovation Team and Outstanding Scholar Program in Guangxi Colleges and Universities, the “139” Projects for Training of High-level Medical Science Talents from Guangxi, the Key Research and Development Project of Guangxi (AB20297009, AA18221001, AB18050020), the Key Laboratory of Early Prevention and Treatment for Regional High-Frequency Tumors of the Ministry of Education, the Guangxi Independent Research Project (GKE2019-ZZ07, GKE-ZZ202005, GKE-ZZ202111), and the Development and Application of Medical and Health Appropriate Technology in Guangxi (S2019039).

Disclosure

The authors report no conflicts of interest.

References

- Sung H, Ferlay J, Siegel RL, et al. Global cancer statistics 2020: GLOBOCAN estimates of incidence and mortality worldwide for 36 cancers in 185 countries. *CA Cancer J Clin*. 2021;71(3):209–249. doi:10.3322/caac.21660
- Tabrizian P, Jibara G, Shrager B, Schwartz M, Roayaie S. Recurrence of hepatocellular cancer after resection: patterns, treatments, and prognosis. *Ann Surg*. 2015;261(5):947–955. doi:10.1097/SLA.0000000000000710
- Wang S, Sun H, Xie Z, et al. Improved survival of patients with hepatocellular carcinoma and disparities by age, race, and socioeconomic status by decade, 1983–2012. *Oncotarget*. 2016;7(37):59820–59833. doi:10.18632/oncotarget.10930
- Zhou J, Sun H, Wang Z, et al. Guidelines for the diagnosis and treatment of hepatocellular carcinoma (2019 edition). *Liver Cancer*. 2020;9(6):682–720. doi:10.1159/000509424
- Heinrich S, Craig AJ, Ma L, Heinrich B, Greten TF, Wang XW. Understanding tumour cell heterogeneity and its implication for immunotherapy in liver cancer using single-cell analysis. *J Hepatol*. 2021;74(3):700–715. doi:10.1016/j.jhep.2020.11.036
- Sun Y, Kucej M, Fan HY, Yu H, Sun QY, Zou H. Separase is recruited to mitotic chromosomes to dissolve sister chromatid cohesion in a DNA-dependent manner. *Cell*. 2009;137(1):123–132. doi:10.1016/j.cell.2009.01.040
- Finetti P, Guille A, Adelaide J, Birnbaum D, Chaffanet M, Bertucci F. ESPL1 is a candidate oncogene of luminal B breast cancers. *Breast Cancer Res Treat*. 2014;147(1):51–59. doi:10.1007/s10549-014-3070-z
- Liu Z, Lian X, Zhang X, et al. ESPL1 is a novel prognostic biomarker associated with the malignant features of glioma. *Front Genet*. 2021;12:666106. doi:10.3389/fgene.2021.666106
- Yang Q, Yu B, Sun J, Huang G. TTK, CDC25A, and ESPL1 as prognostic biomarkers for endometrial cancer. *Biomed Res Int*. 2020;2020:4625123. doi:10.1155/2020/4625123
- Wang R, Zang W, Hu B, et al. Serum ESPL1 can be used as a biomarker for patients with hepatitis B virus-related liver cancer: a Chinese case-control study. *Technol Cancer Res Treat*. 2020;19:1533033820980785. doi:10.1177/1533033820980785
- Nie Z, Pu T, Han Z, et al. Extra spindle pole bodies-like 1 serves as a prognostic biomarker and promotes lung adenocarcinoma metastasis. *Front Oncol*. 2022;12:930647. doi:10.3389/fonc.2022.930647
- Tang Z, Li C, Kang B, Gao G, Li C, Zhang Z. GEPIA: a web server for cancer and normal gene expression profiling and interactive analyses. *Nucleic Acids Res*. 2017;45(W1):W98–w102. doi:10.1093/nar/gkx247
- Ullah M, Han K, Hadi F, Xu J, Song J, Yu DJ. PScL-HDeep: image-based prediction of protein subcellular location in human tissue using ensemble learning of handcrafted and deep learned features with two-layer feature selection. *Brief Bioinform*. 2021;22(6). doi:10.1093/bib/bbab278
- Gao J, Aksoy BA, Dogrusoz U, et al. Integrative analysis of complex cancer genomics and clinical profiles using the cBioPortal. *Sci Signal*. 2013;6(269):pl1. doi:10.1126/scisignal.2004088
- Liu CJ, Hu FF, Xia MX, Han L, Zhang Q, Guo AY. GSCALite: a web server for gene set cancer analysis. *Bioinformatics*. 2018;34(21):3771–3772. doi:10.1093/bioinformatics/bty411
- Zheng C, Zheng L, Yoo JK, et al. Landscape of infiltrating T cells in liver cancer revealed by single-cell sequencing. *Cell*. 2017;169(7):1342–1356. e1316. doi:10.1016/j.cell.2017.05.035
- Sun D, Wang J, Han Y, et al. TISCH: a comprehensive web resource enabling interactive single-cell transcriptome visualization of tumor microenvironment. *Nucleic Acids Res*. 2021;49(D1):D1420–d1430. doi:10.1093/nar/gkaa1020

18. Doncheva NT, Morris JH, Gorodkin J, Jensen LJ. Cytoscape StringApp: network analysis and visualization of proteomics data. *J Proteome Res*. 2019;18(2):623–632. doi:10.1021/acs.jproteome.8b00702
19. Ruan GT, Xie HL, Zhu LC, et al. Immune ULBP1 is elevated in colon adenocarcinoma and predicts prognosis. *Front Genet*. 2022;13:762514. doi:10.3389/fgene.2022.762514
20. Su Y, Chen D, Yuan D, et al. Multi-omics resolves a sharp disease-state shift between mild and moderate COVID-19. *Cell*. 2020;183(6):1479–1495. e1420. doi:10.1016/j.cell.2020.10.037
21. Sun Y, Wu L, Zhong Y, et al. Single-cell landscape of the ecosystem in early-relapse hepatocellular carcinoma. *Cell*. 2021;184(2):404–421.e416. doi:10.1016/j.cell.2020.11.041
22. Hu B, Huang W, Wang R, et al. High rate of detection of human ESPL1-HBV S fusion gene in patients with HBV-related liver cancer: a Chinese case-control study. *Anticancer Res*. 2020;40(1):245–252. doi:10.21873/anticancer.13946
23. Deng Z, Xiao M, Du D, et al. DNASE1L3 as a prognostic biomarker associated with immune cell infiltration in cancer. *Onco Targets Ther*. 2021;14:2003–2017. doi:10.2147/OTT.S294332
24. Yang Y, Ren P, Liu X, et al. PPP1R26 drives hepatocellular carcinoma progression by controlling glycolysis and epithelial-mesenchymal transition. *J Exp Clin Cancer Res*. 2022;41(1):101. doi:10.1186/s13046-022-02302-8
25. Chen M, Zhang C, Liu W, Du X, Liu X, Xing B. Long noncoding RNA LINC01234 promotes hepatocellular carcinoma progression through orchestrating aspartate metabolic reprogramming. *Mol Ther*. 2022;30(6):2354–2369. doi:10.1016/j.ymthe.2022.02.020
26. Prinzhorn W, Stehle M, Kleiner H, et al. c-MYB is a transcriptional regulator of ESPL1/Separase in BCR-ABL-positive chronic myeloid leukemia. *Biomark Res*. 2016;4:5. doi:10.1186/s40364-016-0059-2
27. Wang D, Zhu H, Guo M, et al. Expression and prognostic value of cell-cycle-associated genes in gastric adenocarcinoma. *BMC Gastroenterol*. 2018;18(1):81. doi:10.1186/s12876-018-0811-1
28. Canavese M, Santo L, Raje N. Cyclin dependent kinases in cancer: potential for therapeutic intervention. *Cancer Biol Ther*. 2012;13(7):451–457. doi:10.4161/cbt.19589
29. Kciuk M, Gielecińska A, Mujwar S, Mojzych M, Kontek R. Cyclin-dependent kinases in DNA damage response. *Biochim Biophys Acta Rev Cancer*. 2022;1877(3):188716. doi:10.1016/j.bbcan.2022.188716
30. Tipton AR, Wren JD, Daum JR, Siefert JC, Gorbsky GJ. GTSE1 regulates spindle microtubule dynamics to control Aurora B kinase and Kif4A chromokinesin on chromosome arms. *J Cell Biol*. 2017;216(10):3117–3132. doi:10.1083/jcb.201610012
31. Lin F, Xie YJ, Zhang XK, et al. GTSE1 is involved in breast cancer progression in p53 mutation-dependent manner. *J Exp Clin Cancer Res*. 2019;38(1):152. doi:10.1186/s13046-019-1157-4
32. Guo L, Zhang S, Zhang B, et al. Silencing GTSE-1 expression inhibits proliferation and invasion of hepatocellular carcinoma cells. *Cell Biol Toxicol*. 2016;32(4):263–274. doi:10.1007/s10565-016-9327-z
33. Wu X, Wang H, Lian Y, et al. GTSE1 promotes cell migration and invasion by regulating EMT in hepatocellular carcinoma and is associated with poor prognosis. *Sci Rep*. 2017;7(1):5129. doi:10.1038/s41598-017-05311-2
34. Nakamura T, Furukawa Y, Nakagawa H, et al. Genome-wide cDNA microarray analysis of gene expression profiles in pancreatic cancers using populations of tumor cells and normal ductal epithelial cells selected for purity by laser microdissection. *Oncogene*. 2004;23(13):2385–2400. doi:10.1038/sj.onc.1207392
35. Shimo A, Nishidate T, Ohta T, Fukuda M, Nakamura Y, Katagiri T. Elevated expression of protein regulator of cytokinesis 1, involved in the growth of breast cancer cells. *Cancer Sci*. 2007;98(2):174–181. doi:10.1111/j.1349-7006.2006.00381.x
36. Kanehira M, Katagiri T, Shimo A, et al. Oncogenic role of MPHOSPH1, a cancer-testis antigen specific to human bladder cancer. *Cancer Res*. 2007;67(7):3276–3285. doi:10.1158/0008-5472.CAN-06-3748
37. Chen J, Rajasekaran M, Xia H, et al. The microtubule-associated protein PRC1 promotes early recurrence of hepatocellular carcinoma in association with the Wnt/β-catenin signalling pathway. *Gut*. 2016;65(9):1522–1534. doi:10.1136/gutjnl-2015-310625
38. Zhao Z, Wang Z, Bao ZS, et al. Mutation and copy number alterations analysis of KIF23 in glioma. *Front Genet*. 2021;12:646929. doi:10.3389/fgene.2021.646929
39. Liang WT, Liu XF, Huang HB, Gao ZM, Li K. Prognostic significance of KIF23 expression in gastric cancer. *World J Gastrointest Oncol*. 2020;12(10):1104–1118. doi:10.4251/wjgo.v12.i10.1104
40. Cheng C, Wu X, Shen Y, Li Q. KIF14 and KIF23 promote cell proliferation and chemoresistance in HCC cells, and predict worse prognosis of patients with HCC. *Cancer Manag Res*. 2020;12:13241–13257. doi:10.2147/CMAR.S285367
41. Bai X, Cao Y, Yan X, et al. Systematic pan-cancer analysis of KIF23 and a prediction model based on KIF23 in Clear Cell Renal Cell Carcinoma (ccRCC). *Pharmgenomics Pers Med*. 2021;14:1717–1729. doi:10.2147/PGPM.S337695
42. Jain M, Zhang L, He M, Zhang YQ, Shen M, Kebebew E. TOP2A is overexpressed and is a therapeutic target for adrenocortical carcinoma. *Endocr Relat Cancer*. 2013;20(3):361–370. doi:10.1530/ERC-12-0403
43. Kim EJ, Lee YS, Kim YJ, et al. Clinical implications and prognostic values of topoisomerase-II alpha expression in primary non-muscle-invasive bladder cancer. *Urology*. 2010;75(6):1516.e1519–1513. doi:10.1016/j.urology.2009.08.055
44. Zeng S, Liu A, Dai L, et al. Prognostic value of TOP2A in bladder urothelial carcinoma and potential molecular mechanisms. *BMC Cancer*. 2019;19(1):604. doi:10.1186/s12885-019-5814-y
45. Gao Y, Zhao H, Ren M, et al. TOP2A promotes tumorigenesis of high-grade serous ovarian cancer by regulating the TGF-β/Smad pathway. *J Cancer*. 2020;11(14):4181–4192. doi:10.7150/jca.42736
46. Wang T, Lu J, Wang R, Cao W, Xu J. TOP2A promotes proliferation and metastasis of hepatocellular carcinoma regulated by miR-144-3p. *J Cancer*. 2022;13(2):589–601. doi:10.7150/jca.64017
47. Massagué J. G1 cell-cycle control and cancer. *Nature*. 2004;432(7015):298–306. doi:10.1038/nature03094

International Journal of General Medicine

Dovepress

Publish your work in this journal

The International Journal of General Medicine is an international, peer-reviewed open-access journal that focuses on general and internal medicine, pathogenesis, epidemiology, diagnosis, monitoring and treatment protocols. The journal is characterized by the rapid reporting of reviews, original research and clinical studies across all disease areas. The manuscript management system is completely online and includes a very quick and fair peer-review system, which is all easy to use. Visit <http://www.dovepress.com/testimonials.php> to read real quotes from published authors.

Submit your manuscript here: <https://www.dovepress.com/international-journal-of-general-medicine-journal>